Journal of Hazardous Materials 194 (2011) 79–84

Contents lists available at ScienceDirect

Journal of Hazardous Materials

journal homepage: www.elsevier.com/locate/jhazmat

The recycling of Mn–Zn ferrite wastes through a hydrometallurgical route

Kangkang Li, Changhong Peng*, Kaiqi Jiang

School of Metallurgical Science and Engineering, Central South University, Changsha 410083, PR China

ARTICLE INFO

Article history:
Received 19 April 2011
Received in revised form 19 July 2011
Accepted 20 July 2011
Available online 5 August 2011

Keywords:
Mn–Zn ferrite waste
Recycle
Wet chemical method
Mn–Zn ferrite product

ABSTRACT

A novel recycling route using acid leaching, reduction, purification, co-precipitation and traditional ceramic process was applied to process the Mn–Zn ferrite wastes and prepare the corresponding high permeability soft magnetic product. Above 95% of Fe, Mn, Zn in the waste materials could be recycled in the form of Mn–Zn ferrite products through the hydrometallurgical route. The comprehensive properties of Mn–Zn ferrite prepared from wastes by this route have broader frequency characteristics, higher resistivity, lower loss coefficient and temperature coefficient as compared to the A102 product (Acme Electronics Corporation, Taiwan). Moreover, the cost of this recycling technology has economical advantage over the traditional ceramic process, which holds a promising industrial application.

1. Introduction

Mn–Zn ferrites are ceramic materials applied extensively in transformers, magnetic recording heads, information storage systems, medical diagnostics and biomedicine [1,2], due to their excellent properties such as high magnetic permeability, high saturation magnetization, high dielectric resistivity and low power losses [3–6]. With the development of modern electronic and telecommunications industry, more than 250,000 tons of Mn–Zn ferrites have been annually produced since 2008 in China. This has resulted large amount of waste from discarded Mn–Zn ferrites and grinding products from preparation and processing of the soft ferrites. Some of the wastes are incinerated or buried together with municipal domestic waste; some others are exposed to the nature by simple disposal. Because of the high grades of iron, zinc and manganese, effective utilization of Mn–Zn ferrite wastes has thus become an attractive study from the viewpoint of environmental preservation, resource saving and waste volume reduction.

Mn–Zn ferrites are usually prepared by pressing a pre-sintered mixture of powders containing specific proportion of Fe_2O_3, Mn_3O_4, ZnO to obtain the required shape and then converting it into a magnetic ceramic component by sintering [7,8]. There are some disadvantages inherently associated with this traditional ceramic technology, for instances, the difficulty to obtain chemical homogeneities down to the molecular level and obtain sufficiently dense microstructures at very small grain sizes [8]. Nevertheless, Mn–Zn ferrites of smaller size, more diversity and higher performance are needed by modern science and technology. In order to overcome the limitations arising from the ceramic route, the preparation of Mn–Zn ferrites by wet chemical synthesis routes has been employed. Various wet chemical methods such as co-precipitation [9–11], hydrothermal synthesis [12,13], sol–gel [14,15], microemulsion [16,17] and microwave hydrothermal reaction [18], have been studied. Among these preparation techniques, co-precipitation is considered as a very perspective method, which can give high product purity and homogeneity, fast reaction, regular particle size, narrow distribution range, using simple equipment with low energy requirement [9,19]. The co-precipitation method was also applied to recycle spent Zn–Mn batteries [20,21]. Xi et al. [22] prepared manganese–zinc ferrites by co-precipitation method using spent Zn–Mn batteries and determined the suitable co-precipitation conditions: pH value 7–7.5, temperature 50 °C and calcining temperature 1100–1150 °C. Kim et al. [23] synthesized Mn–Zn ferrite powder with saturation magnetizations of 39–91 emu/g through reductive acid leaching of spent zinc–carbon batteries and oxidative precipitation. However, the study on co-precipitation using Mn–Zn ferrite wastes as raw materials to prepare soft magnetic material has not been reported previously.

In the present work, a novel recycling process of high permeability Mn–Zn ferrite wastes using acid leaching, reduction, purification, co-precipitation, followed by traditional ceramic process, is investigated. The objective of this recycling technology is to turn the Mn–Zn ferrite wastes into the corresponding soft magnetic product, which realizes the environmental and economic benefits.

* Corresponding author. Tel.: +86 731 88836940.
E-mail address: phc416@csu.edu.cn (C. Peng).

0304-3894/$ – see front matter © 2011 Elsevier B.V. All rights reserved.
doi:10.1016/j.jhazmat.2011.07.060

Table 1
Composition of main elements and impurities in the Mn–Zn ferrite waste.

Elements	Fe	Mn	Zn	Si	Ca	Mg
Composition (%)	46.30	11.37	10.64	0.0198	0.0513	0.0127

2. Materials and methods

2.1. Mn–Zn ferrite waste

Mn–Zn ferrite waste is mainly composed of $ZnFe_2O_4$, $MnFe_2O_4$ and Fe_3O_4. Table 1 shows the composition of major components and impurities of high permeability Mn–Zn ferrite waste from Acme Electronics Corporation, Guangdong, China. The process flow diagram for recycling of Mn–Zn ferrite wastes using a combination of hydrometallurgical process and traditional ceramic process is shown in Fig. 1. Conditions used in each unit operation are listed in Table 2.

2.2. Experimental procedure

2.2.1. Sulfuric acid leaching

Sulfuric acid leaching was conducted for extracting major component from the industrial Mn–Zn ferrite wastes. The leaching process was carried out in glass reactor where the diameter and height are 18 cm and 27 cm, respectively. The dosage of sulfuric acid was theoretically determined based on the Fe, Mn and Zn contents in the waste (Table 1). The experimental/theoretical (E/T) ratio of acid dosage was varied in the range 1.0–1.2 (Table 2). The leaching temperature, duration and liquid/solid ratio were varied in the range 80–100 °C, 1–5 h and 2:1–6:1, respectively (Table 2). Agitation speed was 300 rpm.

2.2.2. Reduction

Iron(III) in the leach liquor was reduced by Fe, Mn and Zn powder. The dosage of Fe, Mn and Zn powders was accurately calculated according to the Fe(III), Mn(II) and Zn(II) concentrations in the leachate to assure the molar ratio to reach Fe_2O_3:MnO:ZnO = 52.8:24.2:23.0 relevant to the formula of high permeability Mn–Zn ferrite. The reductive powders were consecutively added into the extraction liquid at 50 °C, following the order of Fe, Zn and Mn according to the reactivity of the three metals, and the reaction time was 1.0 h, 0.5 h and 0.5 h, respectively.

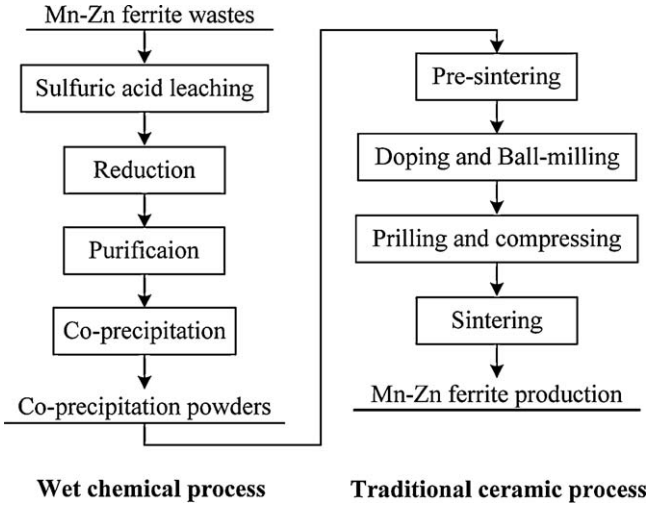

Fig. 1. Process flow sheet for recycling of Mn–Zn ferrite wastes.

2.2.3. Purification

Because of impurities existed in the waste, such as calcium, silicon and magnesium (Table 1), which have a great effect on the magnetization properties of Mn–Zn ferrite products [24–26], it is necessary to remove these impurities before co-precipitation in order to obtain high quality powder. In this process, the removal of Si, Ca and Mg was conducted in a two stage process.

The first stage was desilication with $Fe_2(SO_4)_3$ and $NH_3{\cdot}H_2O$ (5%) at 45 °C. The controlled factors included the $Fe_2(SO_4)_3$ dosage expressed by Fe/Si ratio of 6–24, pH range 3.5–5.0 and reaction time 1.5–3.0 h (Table 2). The second stage was removal of Ca^{2+} and Mg^{2+} with NH_4F and $NH_3{\cdot}H_2O$ (5%). Reaction time was 2.0 h with the E/T ratio of NH_4F dosage (ratio of 4–24 and reaction temperature in the range 45–75 °C at pH 2.5–5.0 (Table 2).

2.2.4. Co-precipitation

Co-precipitation was carried out with $NH_4HCO_{3(s)}$ for 2.0 h at 50 °C. The $NH_4HCO_{3(s)}$ was added continuously until the pH of liquid reached about 7.0. The precipitate was filtered, and washed several times with distilled water to remove SO_4^{2-}, and then dried at 105 °C for 4.0 h.

2.2.5. Production of Mn–Zn ferrite

Steps relevant to the traditional ceramic process of Mn–Zn ferrite using co-precipitation powder were followed: (I) pre-sintering in the muffle at 850 °C for 3.0 h, (II) doping with MoO_3 (400 ppm), Bi_2O_3 (350 ppm), SnO_2 (150 ppm), (III) milling for 9.0 h in the dual planetary ball mills, (IV) manual granulation with 10% PVA, (V) forming a circle ($\Phi 30 \times \Phi 18 \times 9$ mm) with compacting pressure 15 MPa using hydraulic press, and (VI) calcining in the sintering elevator furnace at 1320 °C for 4.0 h with 5.4% partial pressure of oxygen.

2.3. Analytical methods

The contents of various metallic elements in the Mn–Zn ferrite wastes and subsequent products after each operation were determined using ICP Atomic Emission Spectrophotometer (Intrepid II XSP, American). The pH value of the aqueous solution was measured with a pH/mV meter (Model DF-801, China). The permeability of Mn–Zn ferrite was detected by LCR broadband digital bridge (HG2817A, China). The other magnetic parameters were determined using the magnetic property measurement system (Model MPMS XL-7, Quantum Design, America).

3. Results and discussion

3.1. Acid leaching

Effect of variables (Table 2) on sulfuric acid leaching efficiency is shown in Fig. 2. With the increase of sulfuric acid dosage, the leaching efficiency of Fe, Mn and Zn increased sharply and exceeded 92% at E/T ratio of 1.15. However, leaching percentages of the three metals increased slightly when the E/T ratio was between 1.15 and 1.20 (Fig. 2a). The results showed that the E/T ratio of 1.15 is satisfactory for the acid leaching requirement.

The leaching efficiency of Fe, Mn and Zn was significantly affected by the increase in temperature as shown in Fig. 2b. The average leaching percentage of Fe, Mn and Zn increased from 84% at 80 °C to 98% at 95 °C. Although the leaching efficiency of 99.1% at 100 °C was higher than 98.5% at 95 °C, higher temperature causes moisture evaporation and waste more energy, which is unsuitable for industrial production.

The leaching efficiency increased with the extension of time (Fig. 2c). When the leaching time was above 3.0 h, average leach-

Table 2
Conditions used in different unit operations.

Operation	Reagent and dosage	Temperature (°C)	pH	Reaction time (h)	Liquid/solid ratio
Acid leach of ferrite wastes	*E*/*T* ratio of H_2SO_4 acid 1.00, 1.05, 1.10, 1.15, 1.20	80, 85, 90, 95, 100	–	1, 2, 3, 4, 5	2:1, 3:1, 4:1, 5:1, 6:1
Fe(III) reduction with metals	Fe, Mn, Zn powders To maintain ratio Fe_2O_3: 52.8 MnO: 23.0 ZnO: 24.2	50	–	Fe: 1.0 Mn: 0.5 Zn: 0.5	–
Purification step 1: desilication	$Fe_2(SO_4)_3$ and NH_3/H_2O (5%) Fe/Si ratio 6, 12, 18, 24	45	3.5,4.0, 4.5,5.0	1.5, 2.0, 2.5, 3.0	–
Purification step 2: removal of Ca^{2+} and Mg^{2+}	NH_4F and NH_3/H_2O (5%) *E*/*T* ratio 4, 8, 12, 16, 20, 24	45, 55, 65, 75	2.5,3.0, 3.5,4.5, 5.0	2	–
Coprecipitation	$NH_4HCO_{3(s)}$	50	7	2	–

ing efficiency of Fe, Mn and Zn reached 99.0%, with no obvious improvement between 3.0 h and 5.0 h.

The results in Fig. 2d show the increase of liquid/solid ratio has only limited effect on the leaching efficiency at high ratio. Therefore, the optimal leaching time of 3.0 h at *E*/*T* dosage ratio of 1.15 at reaction temperature 95 °C with liquid/solid ratio 4:1 was chosen for economic and water-saving concern.

3.2. Reduction

Iron(III) in the leachate is prone to generate iron hydroxide which is difficult to separate and wash completely due to its small particle size and large specific surface area. Thus, it is necessary to reduce Fe(III) ions to avoid the formation of iron hydroxide colloidal precipitate. The reduction is also a key process to ensure the composition to reach the designed molar ratio of Fe_2O_3:MnO:ZnO = 52.8:24.2:23.0. The dosage and sequence of adding Fe, Zn and Mn powders need strict control although the reaction time presents no obvious influence on reduction efficiency because of the rapid rate. In order to confirm the reproducibility of experiment, the reduction process was repeated 5 times. The concentrations of Fe, Mn and Zn in solution and Fe_2O_3–MnO–ZnO ratio are shown in Table 3. The average relative standard deviation (RSD) of Fe_2O_3, MnO and ZnO was −0.139%, MnO −0.139% and ZnO 0.461%, respectively. The relative error between the designed ratio and actual ratio was in the range of ±0.50%, which satisfied the requirement of industrial Mn–Zn ferrite product (±2.0%). Furthermore, the Fe(III) concentration in the reduction solution was found to be less than 0.1 g L^{-1}, and the reduction efficiency was above 99.8%, indicating that the reduction was performed completely.

3.3. Purification

The effect of *E*/*T* dosage ratio of Fe/Si, reaction time and pH on the Si removal is shown in Fig. 3. A low ratio of Fe/Si, long reaction time and high pH was beneficial for the removal of Si. The removal efficiency reached as high as 81% at Fe/Si 12–18, but decreased at a higher of 24 (Fig. 3a). As shown in Fig. 3b, the removal efficiency increased with increasing pH, and reached a maximum of 80% at pH 4–5. A high pH value of 5.0 has no beneficial effect and may cause

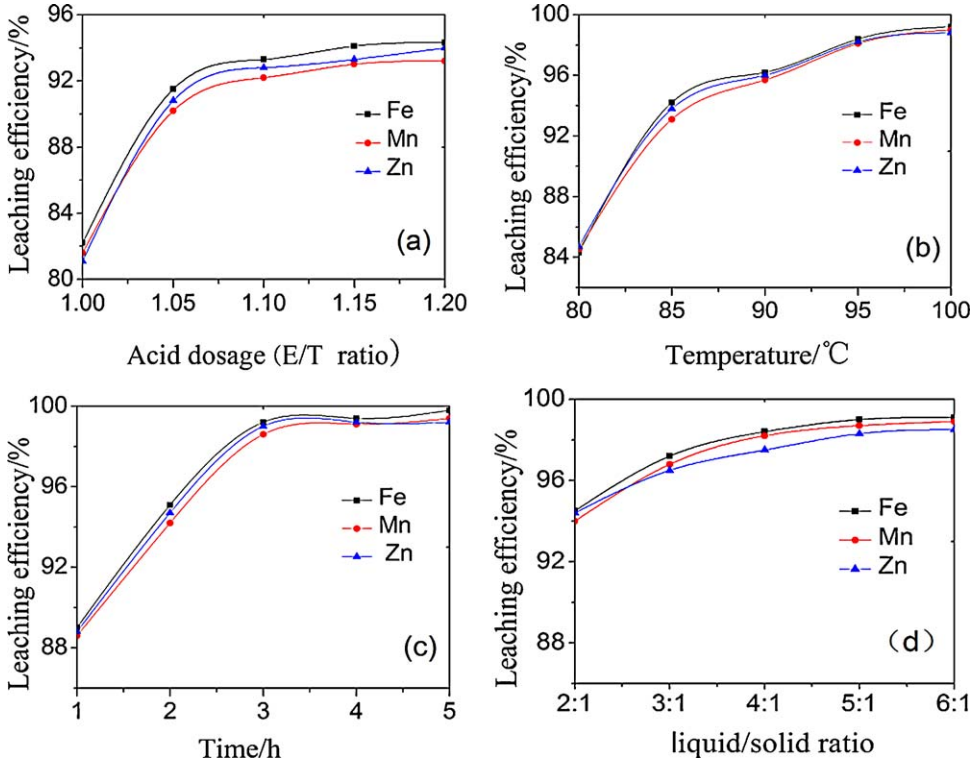

Fig. 2. Effect of different experimental parameters on sulfuric acid leaching efficiency: (a) *E*/*T* ratio (at 80 °C after 3.0 h, liquid/solid ratio 5:1), (b) leaching temperature (*E*/*T* ratio 1.15 after 3.0 h, liquid/solid ratio 5:1), (c) leaching time (*E*/*T* ratio 1.15 at 95 °C, liquid/solid ratio 5:1), and (d) liquid/solid ratio (*E*/*T* ratio 1.15 after 3.0 h at 95 °C).

Table 3
Concentration and ratio of Fe, Mn and Zn in reduction solution.

No.	Major component ($g L^{-1}$)			Actual molar ratio	RSD (%)		
	Fe	Mn	Zn	Fe_2O_3:MnO:ZnO	Fe_2O_3	MnO	ZnO
1	47.36	10.46	12.28	52.84:23.73:23.43	0.076	−1.942	1.869
2	49.79	11.18	12.61	52.93:24.17:22.90	0.233	−0.124	−0.435
3	51.32	11.62	13.28	52.56:24.21:23.23	−0.430	0.041	1.000
4	52.12	11.92	13.35	52.58:24.43:22.99	−0.417	0.958	−0.043
5	53.82	12.20	13.74	52.72:24.29:22.98	−0.156	0.372	−0.087
Average	50.88	11.48	13.05	52.73:24.17:23.10	−0.139	−0.139	0.461

Designed formulation of Mn–Zn ferrite: Fe_2O_3:MnO:ZnO = 52.8:24.2:23.0.

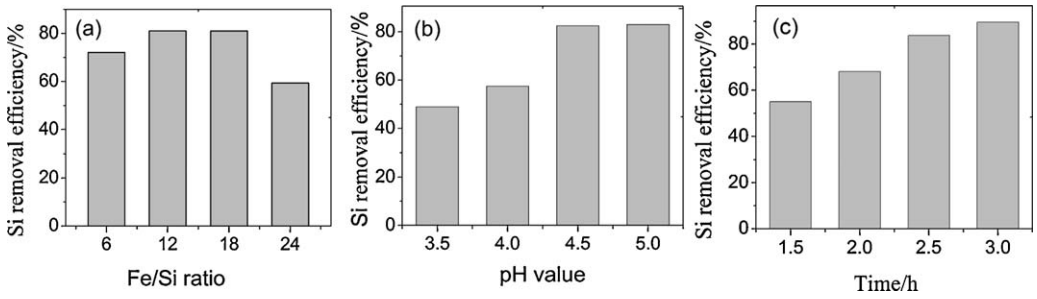

Fig. 3. Effect of different experimental parameters on desilication: (a) Fe/Si ratio (pH 4.0 after 2.0 h), (b) pH value (Fe/Si ratio 12 after 2.0 h), and (c) reaction time (Fe/S ratio 12, pH 4.5).

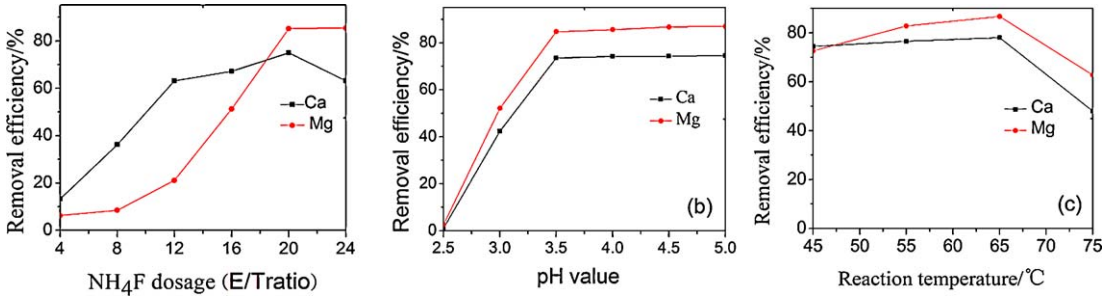

Fig. 4. Effect of different experimental parameters on removal of Ca^{2+} and Mg^{2+}: (a) *E*/*T* ratio (at 45 °C; pH 4.0), (b) pH value (*E*/*T* ratio 20; *T* 45 °C), and (c) reaction temperature (*E*/*T* ratio 20; pH 3.5).

the losses of major component due to the formation of $Fe(OH)_2$, $Zn(OH)_2$ and $Mn(OH)_2$. The removal efficiency of Si increased over the time, indicating that the equilibrium of Si adsorption onto ferrihydrite is a slow process removing >90% Si after 3 h (Fig. 3c). The optimal conditions of the hydrolysis purification process are $Fe_2(SO_4)_3$ dosage of Fe/Si ratio 12, pH 4.5 and a reaction time of 3 h.

The effect of variables on the removal of Ca^{2+}/Mg^{2+} by the precipitation reaction $M^{2+} + F^- = MF_2(s)$ (M = Ca, Mg) is shown in Fig. 4.The maximum Ca, Mg removal efficiency reach 74.8%, 85.8%, respectively, when the *E*/*T* ratio of NH_4F dosage is 20 (Fig. 4a). Removal efficiency was greatly enhanced with the increasing pH between 2.5 and 3.5, but pH >3.5 has no effect on the removal of Ca and Mg (Fig. 5b). Temperature in the range 45–65 °C can improve purification efficiency, but higher temperature (75 °C) has lower removal efficiency (Fig. 5c). Therefore, the optimal conditions of fluorination process are *E*/*T* ratio of NH_4F dosage 20, pH 3.5 and reaction temperature 65 °C.

3.4. Co-precipitation

To ensure the complete precipitation of Fe(II), Mn(II) and Zn(II) in the purified leach liquor, the pH value should be strictly controlled during co-precipitation process. Table 4 shows the possible reactions and equilibrium constants [27] in the system of Fe(II)–Mn(II)–Zn(II)–NH_4HCO_3–H_2O. The total concentrations of Zn(II), Fe(II) and Mn(II) are expressed as $[Fe]_T$, $[Zn]_T$, $[Mn]_T$, respectively and calculated as follows:

$$[Fe]_T = [Fe^{2+}] + [Fe(OH)^+] + [Fe(OH)_2] + [Fe(OH)_3^-] + [Fe(OH)_4^{2-}]$$

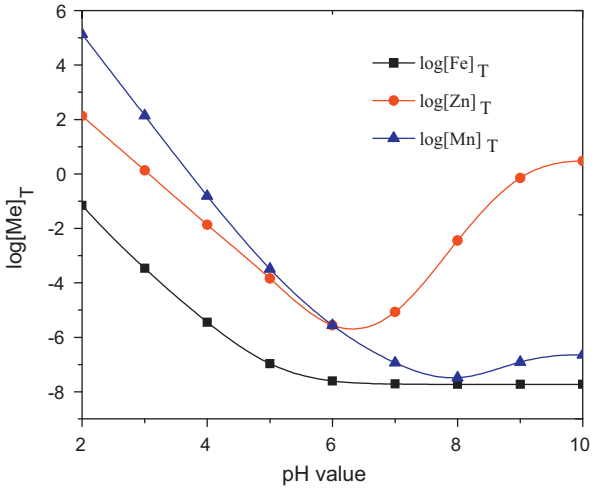

Fig. 5. Effect of pH on calculated solubility of metal ions at 298 K.

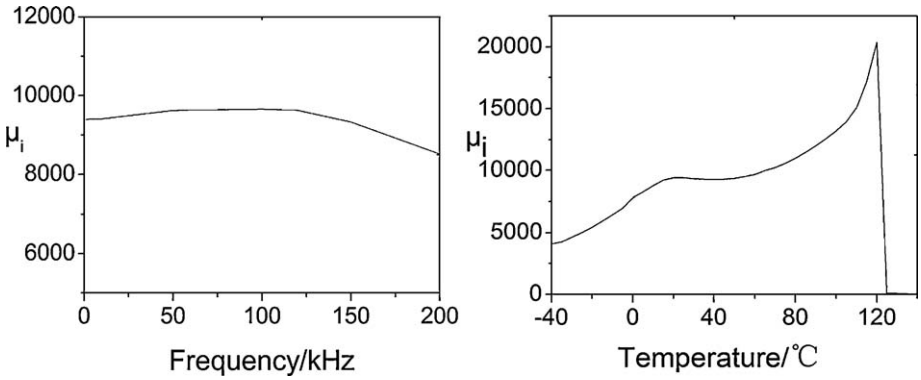

Fig. 6. The performance of Mn–Zn ferrite production: (a) frequency characteristic, (b) temperature characteristic.

Table 4
Possible reactions in co-precipitation in accordance with their equilibrium constants.

No.	Reaction	Equilibrium constant [27]
1	$HCO_3^- \rightleftharpoons H^+ + CO_3^{2-}$	−10.3
2	$H_2CO_3 \rightleftharpoons H^+ + HCO_3^-$	−6.35
3	$Fe^{2+} + CO_3^{2-} \rightleftharpoons FeCO_{3(S)}$	10.5
4	$Mn^{2+} + CO_3^{2-} \rightleftharpoons MnCO_{3(S)}$	9.30
5	$Zn^{2+} + CO_3^{2-} \rightleftharpoons ZnCO_{3(S)}$	10.8
6	$Fe(OH)^+ \rightleftharpoons Fe^{2+} + OH^-$	−4.50
7	$Fe(OH)_2 \rightleftharpoons Fe^{2+} + 2OH^-$	−7.40
8	$Fe(OH)_3^- \rightleftharpoons Fe^{2+} + 3OH^-$	−10.0
9	$Fe(OH)_4^{2-} \rightleftharpoons Fe^{2+} + 4OH^-$	−9.60
10	$Fe^{2+} + 2OH^- \rightleftharpoons Fe(OH)_{2(S)}$	15.1
11	$Mn(OH)^+ \rightleftharpoons Mn^{2+} + OH^-$	−3.40
12	$Mn(OH)_4^{2-} \rightleftharpoons Mn^{2+} + 4OH^-$	−7.70
13	$Mn_2(OH)^{3+} \rightleftharpoons 2Mn^{2+} + OH^-$	−3.40
14	$Mn_2(OH)_3^+ \rightleftharpoons 2Mn^{2+} + 3OH^-$	−18.1
15	$Mn^{2+} + 2OH^- \rightleftharpoons Mn(OH)_{2(S)}$	12.8
16	$Zn(OH)^+ \rightleftharpoons Zn^{2+} + OH^-$	−5.00
17	$Zn(OH)_2 \rightleftharpoons Zn^{2+} + 2OH^-$	−11.1
18	$Zn(OH)_3^- \rightleftharpoons Zn^{2+} + 3OH^-$	−13.6
19	$Zn(OH)_4^{2-} \rightleftharpoons Zn^{2+} + 4OH^-$	−14.8
20	$Zn^{2+} + 2OH^- \rightleftharpoons Zn(OH)_{2(S)}$	16.2
21	$NH_4^+ \rightleftharpoons NH_3 + H^+$	−9.24
22	$Mn(NH_3)^{2+} \rightleftharpoons Mn^{2+} + NH_3$	−1.00
23	$Mn(NH_3)_2^{2+} \rightleftharpoons Mn^{2+} + 2NH_3$	−1.54
24	$Mn(NH_3)_3^{2+} \rightleftharpoons Mn^{2+} + 3NH_3$	−1.70
25	$Mn(NH_3)_4^{2+} \rightleftharpoons Mn^{2+} + 4NH_3$	−1.30
26	$Zn(NH_3)^{2+} \rightleftharpoons Zn^{2+} + NH_3$	−2.21
27	$Zn(NH_3)_2^{2+} \rightleftharpoons Zn^{2+} + 2NH_3$	−4.50
28	$Zn(NH_3)_3^{2+} \rightleftharpoons Zn^{2+} + 3NH_3$	−6.86
29	$Zn(NH_3)_4^{2+} \rightleftharpoons Zn^{2+} + 4NH_3$	−8.89

$$[Mn]_T = [Mn^{2+}] + [Mn(OH)^+] + [Mn(OH)_4^{2-}] + [Mn_2(OH)^{3+}] + [Mn_2(OH)_3^+] + [Mn(NH_3)^{2+}] + [Mn(NH_3)_2^{2+}] + [Mn(NH_3)_3^{2+}] + [Mn(NH_3)_4^{2+}]$$

$$[Zn]_T = [Zn^{2+}] + [Zn(OH)^+] + [Zn(OH)_2] + [Zn(OH)_3^-] + [Zn(OH)_4^{2-}] + [Zn(NH_3)^{2+}] + [Zn(NH_3)_2^{2+}] + [Zn(NH_3)_3^{2+}] + [Zn(NH_3)_4^{2+}]$$

The concentration of each species at different pH values was calculated using the values of equilibrium constant in Table 4. Results in Fig. 5 shows that $[Zn]_T$, $[Fe]_T$ and $[Mn]_T$ have minimal values in the pH range of 6–7, implying that controlling pH between 6 and 7 may ensure their complete co-precipitation. The pH of co-precipitation was controlled at 6.8 in this process. The experiments were repeated three times, and the average co-precipitation efficiency of Fe, Mn and Zn reached 99.0%, 99.3%, 98.6%, respectively, confirming complete precipitation.

3.5. Characteristics of Mn–Zn ferrite

High permeability Mn–Zn ferrite was obtained through traditional ceramic process in combination of pre-sintering, doping, milling, granulating, forming and sintering (Fig. 1). Table 5 compares the characteristics of the Mn–Zn ferrite produced in this study with the A102 product made by Acme Electronics Corporation of Taiwan. The comprehensive performances of the high permeability Mn–Zn ferrite prepared through the wet route in the present study have obvious advantages over A102 including broader frequency characteristic, higher resistivity, lower loss coefficient and temperature coefficient. Other performances such as initial permeability, saturation induction density, residual magnetic flux density, are close to A102.

Fig. 6 shows the frequency characteristic and temperature characteristic of the Mn–Zn ferrite production. The initial permeability of ferrite is 10,000 at room temperature (Fig. 6b) and the value is unaffected by the change in frequency 0–150 kHz (Fig. 6a), suggesting that the material has broad frequency characteristics. The

Table 5
Comparison of characteristics of the ferrite prepared in this study and A102 of Acme Electronics Corporation.

Performance			Measure conditions			Production	
Property	Symbol	Unit	Freq. (kHz)	Flux den. (mT)	Temp. (°C)	A102	Prepared
Initial permeability	μ_i	1	–	–	25	10000 ± 30%	9380
Relative loss factor	$tg\delta/\mu_i$	10^{-6}	10	<0.25	25	<10	2.41
Frequency characteristic	–	1	–	–	25	0.88	0.97
Resistivity	ρ	Ω	500	–	25	1858	2082
Curie temperature	T_c	°C	–	–	–	120	120
Temperature factor of permeability	αF	10^{-6}	10	<0.25	0–20	−1.0 to 1.0	−0.2 to 0.5
Saturation flux density	Bms	mT	10	H = 1200 A/m	25	380	394
Remanence	Brms	mT	10	H = 1200 A/m	25	95	70
Density	d	g/cm^3	–	–	–	4.90	5.00

Table 6
Cost of recycling Mn–Zn ferrite waste using a wet chemical route.

	Raw material and manufacturing cost	Cost (dollars/ton)	Note
1	Mn–Zn ferrite waste	131	
2	concentrated sulfuric acid	85	
3	ammonium bicarbonate	284	
4	Mn powder	103	
5	Zn powder	115	
6	Fe powder	97	
7	PVA	28	The market price of high permeability Mn–Zn ferrite precursor is about 2200 dollars
8	Others materials ($Fe_2(SO4)_3$, NH_3H_2O, NH_4F, etc.)	53	
9	Oil (gasoline, diesel)	230	
10	Electricity	200	
11	Water	30	
12	Labour	114	
13	Factory rent	61	
14	Taxation expense	61	
15	Equipment amortization	126	
16	Others	76	
	Total	1794	

magnetic permeability remains unchanged at temperature range 20–80 °C indicating a low temperature coefficient and better adaptability to environment.

3.6. Cost estimation

Based on the pilot plant test of the hydrometallurgical route in KeCheng Corporation, Guangdong, China, the cost of recycling Mn–Zn ferrite wastes by the proposed method in this study is shown in Table 6, indicating that the wet chemical technology has cost advantage over traditional ceramic method.

4. Conclusions

Mn–Zn ferrite waste is used as raw material to prepare the corresponding soft magnetic product via a multi-step route consisting of acid leaching, reduction, purification, co-precipitation and conventional ceramic process. Through the wet chemical method, most of iron, manganese and zinc in the soft ferrite waste were recycled. The combination properties of high permeability Mn–Zn ferrite product have obvious advantages over A102 made in Acme Electronics Corporation of Taiwan.

The hydrometallurgical route not only makes the Mn–Zn ferrite waste reduced, reused and recycled, but also turns the wastes into Mn–Zn ferrite product which has economic value. Furthermore, the cost of this recycling technology in the present study has economical advantage over the traditional ceramic process.

The conventional ceramic process requires further investigation, for instance, doping agent and dosage, pre-sintering conditions, ball-milling factors and sintering characteristic. The novel method can make great use of Mn–Zn ferrite waste, which has obvious environmental and economical benefits.

References

[1] Z. Zheng, X. Zhong, Y. Zhang, H. Yu, D. Zeng, Synthesis, structure and magnetic properties of nanocrystalline $Zn_xMn_{1-x}Fe_2O_4$ prepared by ball milling, J. Alloys Compd. 466 (2008) 377–382.
[2] S. Dasgupta, K.B. Kim, J. Ellrich, J. Eckert, I. Manna, Mechano-chemical synthesis and characterization of microstructure and magnetic properties of nanocrystalline $Mn_{1-x}Zn_xFe_2O_4$, J. Alloys Compd. 424 (2006) 13–20.
[3] G. Ott, J. Wrba, R. Lucke, Recent developments of Mn–Zn ferrites for high permeability applications, J. Magn. Magn. Mater. 254–255 (2003) 535–537.
[4] S. Chen, S. Chang, C. Tsay, K. Liu, I. Lin, Improvement on magnetic power loss of Mn–Zn ferrite materials by V_2O_5 and Nb_2O_5 co-doping, J. Eur. Ceram. Soc. 21 (2001) 1931–1935.
[5] P. Hu, H. Yang, D. Pan, H. Wang, Heat treatment effects on microstructure and magnetic properties of Mn–Zn ferrite powders, J. Magn. Magn. Mater. 322 (2010) 173–177.
[6] Y. Liu, J. Cao, Z. Yang, The structure and magnetic properties of Mn–Zn ferrite thin films fabricated by alternately sputtering, Mater. Sci. Eng. B 127 (2006) 108–111.
[7] M. Gua, G. Liu, W. Wang, Study of Mn_3O_4 doping to improve the magnetic properties of MnZn ferrites, Mater. Sci. Eng. B 158 (2009) 35–39.
[8] L. Nalbandian, A. Delimitis, V.T. Zaspalis, E.A. Deliyanni, D.N. Bakoyannakis, E.N. Peleka, Hydrothermally prepared nanocrystalline Mn–Zn ferrites: synthesis and characterization, Micropor. Mesopor. Mater. 114 (2008) 465–473.
[9] R. Arulmurugan, B. Jeyadevan, G. Vaidyanathan, S. Sendhilnathan, Effect of zinc substitution on Co–Zn and Mn–Zn ferrite nanoparticles prepared by co-precipitation, J. Magn. Magn. Mater. 288 (2005) 470–477.
[10] R. Arulmurugan, G. Vaidyanathan, S. Sendhilnathan, B. Jeyadevan, Mn–Zn ferrite nanoparticles for ferrofluid preparation: study on thermal-magnetic properties, J. Magn. Magn. Mater. 298 (2006) 83–94.
[11] B. Jeyadevan, K. Tohji, K. Nakatsuka, A. Narayanasamy, Irregular distribution of metal ions in ferrites prepared by co-precipitation technique structure analysis of Mn–Zn ferrite using extended X-ray absorption fine structure, J. Magn. Magn. Mater. 217 (2000) 99–105.
[12] L. Xiao, T. Zhou, J. Meng, Hydrothermal synthesis of Mn–Zn ferrites from spent alkaline Zn–Mn batteries, Particuology 7 (2009) 491–495.
[13] J. Feng, L. Guo, X. Xu, S. Qi, M. Zhang, Hydrothermal synthesis and characterization of $Mn_{1-x}Zn_xFe_2O_4$ nanoparticles, Physica B 394 (2007) 100–103.
[14] P.P. Hankare, R.P. Patil, U.B. Sankpal, S.D. Jadhav, K.M. Garadkar, S.N. Achary, Synthesis and morphological study of chromium substituted Zn-Mn ferrites nanostructures via sol–gel method, J. Alloys Compd. 509 (2011) 276–280.
[15] J. Azadmanjiri, Preparation of Mn–Zn ferrite nanoparticles from chemical sol–gel combustion method and the magnetic properties after sintering, J. Non-Cryst. Solids 353 (2007) 4170–4173.
[16] J. Wang, P. Chong, S. Ng, L. Gan, Microemulsion processing of manganese zinc ferrites, Mater. Lett. 30 (1997) 217–221.
[17] D.S. Mathew, R.S. Juang, An overview of the structure and magnetism of spinel ferrite nanoparticles and their synthesis in microemulsions, Chem. Eng. J. 129 (2007) 51–65.
[18] T. Caillot, G. Pourroy, D. Stuerga, Novel metallic iron/manganese–zinc ferrite nanocomposites prepared by microwave hydrothermal flash synthesis, J. Alloys Compd. 509 (2011) 3493–3496.
[19] C. Zhang, X. Zhong, H. Yu, Z. Liu, D. Zeng, Effects of cobalt doping on the microstructure and magnetic properties of Mn–Zn ferrites prepared by the co-precipitation method, Physica B 404 (2009) 2327–2331.
[20] J. Nan, D. Han, M. Cui, M. Yang, L. Pan, Recycling spent zinc manganese dioxide batteries through synthesizing Zn–Mn ferrite magnetic materials, J. Hazard. Mater. B 133 (2006) 257–261.
[21] C. Peng, B. Bai, Y. Chen, Study on the preparation of Mn–Zn soft magnetic ferrite powders from waste Zn–Mn dry batteries, Waste Manage. 28 (2008) 326–332.
[22] G. Xi, Y. Li, Y. Liu, Study on preparation of manganese–zinc ferrites using spent Zn–Mn batteries, Mater. Lett. 58 (2004) 1164–1167.
[23] T.H. Kim, G. Senanayake, J.G. Kang, J.S. Sohn, K.I. Rhee, S.W. Lee, S.M. Shin, Reductive acid leaching of spent zinc–carbon batteries and oxidative precipitation of Mn–Zn ferrite nanoparticles, Hydrometallurgy 96 (2009) 154–158.
[24] I. Maghsoudi, M.J. Hadianfard, H. Shokrollahi, The influence of Al content and $CaO–SiO_2$ on the magnetic and structural properties of Al-substituted Ni ferrites, J. Alloys Compd. 481 (2009) 539–542.
[25] A.H. Qureshi, The influence of hafnia and impurities (CaO/SiO_2) on the microstructure and magnetic properties of Mn–Zn ferrites, J. Cryst. Growth 286 (2006) 365–370.
[26] H. Shokrollahi, K. Janghorban, Influence of additives on the magnetic properties, microstructure and densification of Mn–Zn soft ferrites, Mater. Sci. Eng. B 141 (2007) 91–107.
[27] R.M. Smith, A.E. Martell, Critical Stability Constants, Plenum Press, New York, 1979.